

Highly Intergrated X-Band LTCC Receiver Module

Bo Zhou*, Qiang Ma, Qipeng Wang, Liwei Yan, Na Zhou, and Chong-Hu Cheng

Abstract—A highly integrated X-band receiver module is designed based on a 10-layered low temperature co-fired ceramic (LTCC) substrate. A compact X-band bandpass filter (BPF), an intermediate frequency (IF) band hybrid and an IF band BPF are proposed for the receiver module. The measured gain parameter of the proposed receiver is higher than 51 dB, and noise figure (NF) and image rejection are better than 2.5 dB and 37 dB, respectively. The overall size of the receiver module is only 54 mm × 15 mm × 1 mm. Comparisons and discussions are also provided.

1. INTRODUCTION

The use of X-band active phased arrays for military detecting applications is becoming more and more important and effective. Radars with active phased array antenna can flexibly detecting any objects by electronic beam steering. In an active phased array system, each antenna element is interconnected with a T/R module. So the effectiveness and compactness of the T/R module are main challenging goals to be met. Driven by the demands for small-size, lightweight and high performance military phased array devices, there is increasing interest in developing compact phased array T/R modules. Recent advances in integration technology and device performance have paved the way for higher integration of System on Chip (SoC) or System-in-Package (Sip). Low-temperature co-fired ceramic (LTCC)-based modules for phased array applications have been designed and implemented in [1-6]. Bucci et al. solved the problem of optimal power-pattern synthesis of circularly symmetric shaped beam in [7].

In this paper, two BPFs and one hybrid are proposed and integrated into a LTCC receiver module, which down converts and amplifies X-band frequency signals to several dozens of megahertz intermediate frequency (IF) band. The overall size of the proposed receiver is only 54 mm × 15 mm × 1 mm.

2. CIRCUIT DESIGN

2.1. Requirements and Block Diagram

Our goal is to design an X-band receiver, which down-converts signals at the center frequency of 9 GHz to the IF band at a center frequency of 60 MHz. The receiver is required to have a gain higher than 50 dB, noise figure (NF) lower than 3 dB and an image rejection higher than 35 dB, respectively. Moreover, the width of the receiver must be about 15 mm, which is half-wavelength distance between adjacent receiver elements when forming phased arrays.

Since size reduction is the main challenge of this work, the first step is to choose an appropriate layout with a minimal number of circuit elements. The proposed diagram is shown in Figure 1. The system is composed of two low noise amplifiers (LNAs), one X-band BPF, one image rejection mixer (IRM), one quadrature hybrid, one IF BPF and one IF amplifier. The LNA chips use HMC902; the IRM uses HMC520; the IF amplifier uses PW112.

The overall path can provide about 51 dB gain.

Received 9 December 2016, Accepted 9 January 2017, Scheduled 26 January 2017

* Corresponding author: Bo Zhou (sarahxboy@hotmail.com).

The authors are with the School of Electronic Science and Engineering, Nanjing University of Posts and Telecommunications, Nanjing 210023, People's Republic of China.

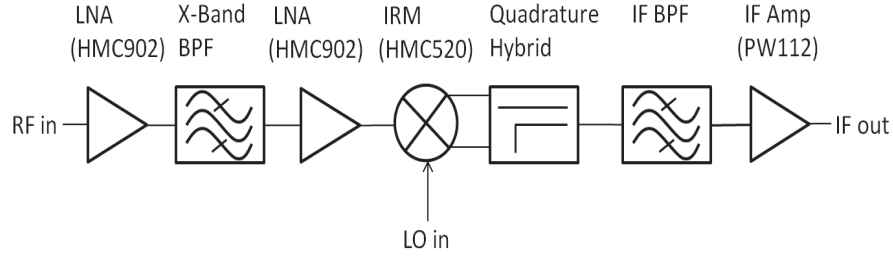


Figure 1. LTCC receiver function diagram.

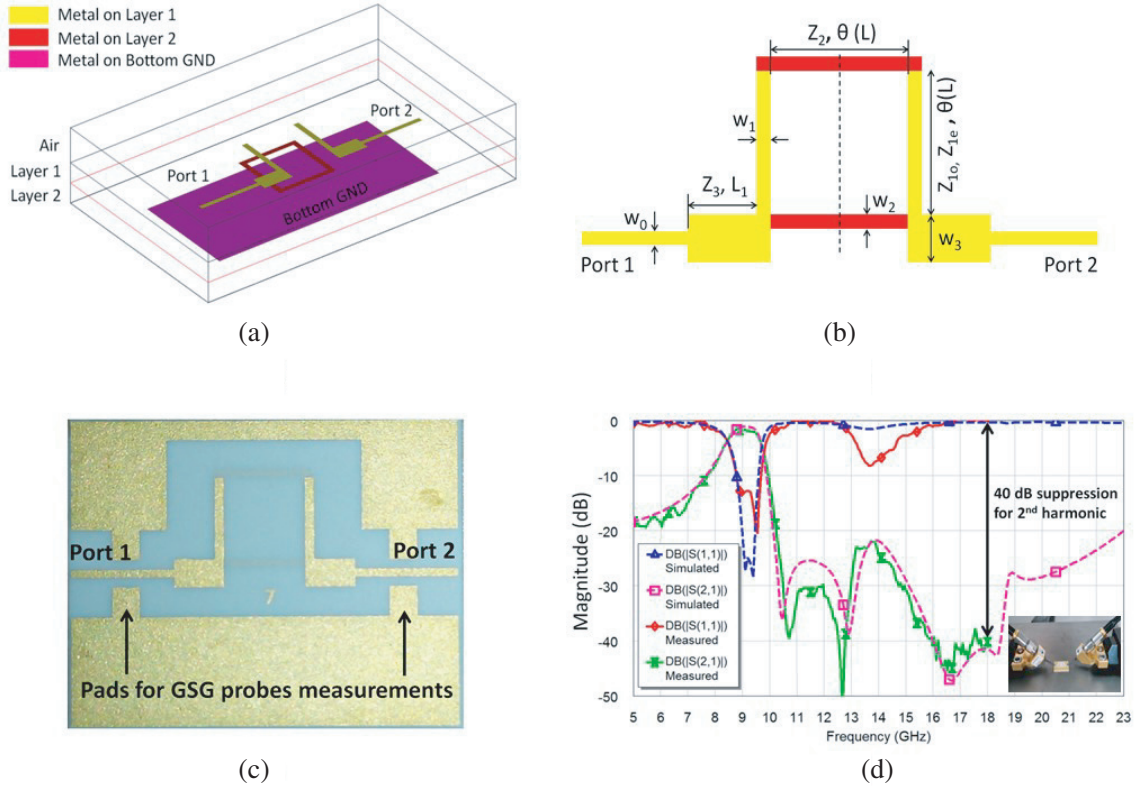


Figure 2. The proposed BPF. (a) Structure, (b) geometry with parameters definitions, (c) photograph and (d) measured S -parameters.

2.2. X-Band BPF Design

Although the dual-mode BPFs with wide upper stopbands have been reported in [8–10], the I/O feed of those BPFs is orthogonal, which is inconvenient for interconnection. Figure 2(a) shows the structure of the proposed wide upper stopband and nonorthogonal I/O feed dual-mode LTCC BPF. The center frequency of the proposed BPF is 9 GHz with a bandwidth of 1 GHz. To realize an enhanced capacitive coupling for a relative wide fractional bandwidth (FBW) of 11%, the square ring resonator is fed by 2-layer broadside parallel-coupled lines. The bottom side of the 2nd-layer is set as ground layer. The 2-layer structure can not only achieve high coupling capacitance, but also gain size reduction using vertical broadside coupled lines instead of planar edge coupled lines. The wide upper stopband is achieved by the stepped impedance microstrip lines near the I/O ports, shown in Figure 2(b). The vertical and horizontal side strips are designed with widths of W_1 and W_2 , respectively. The vertical and horizontal side strips have the same length L . The characteristic impedance of the I/O microstrip lines is 50Ω .

The EM-simulator AWR AXIEM is used to obtain the final optimal parameters. Figure 2(c) shows

a photograph of the proposed BPF. Measurements are carried out by Agilent N5230C network analyzer and Cascade Microtech Summit 9000 probe stations with 400 μm -GSG probes. The measured center frequency is 9 GHz with an FBW of 11%. Measured S_{21} and S_{11} are better than -1.8 and -12 dB in the passband, respectively. 40 dB suppression of $2f_0$ (18 GHz) and a prediction of 20 dB suppression up to $2.4f_0$ (23 GHz) are achieved, shown in Figure 2(d). The size of the proposed BPF is only $7 \times 4 \times 0.2$ mm (without pads for GSG probes). More attentions should be paid to the roughness of top metal layer, which may result in a higher passband insertion loss because of higher resistive loss.

2.3. IF Band Hybrid Design

Moreover, lumped topologies of branch-line coupler in [10] suffered from a narrow fractional bandwidth (FBW) of only $1 \sim 2\%$. Wideband lumped topology for branch-line coupler has been proposed in [11], but it requires comparative high capacitance and inductance, which lead to large size of elements. As the center frequency of IF band is only 60 MHz with a bandwidth of 20 MHz, a wideband lumped-element

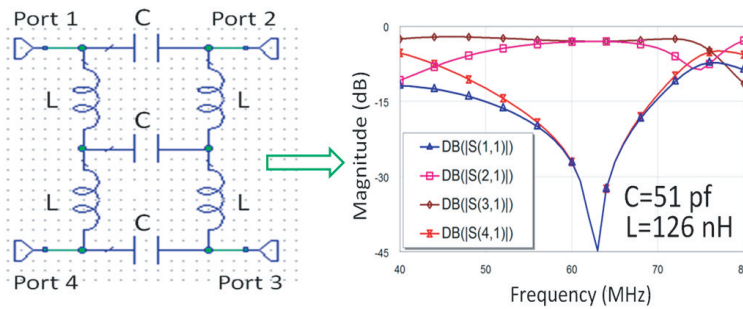


Figure 3. Hybrid's circuit topology with simulated S -parameters for 50 ~ 70 MHz applications.

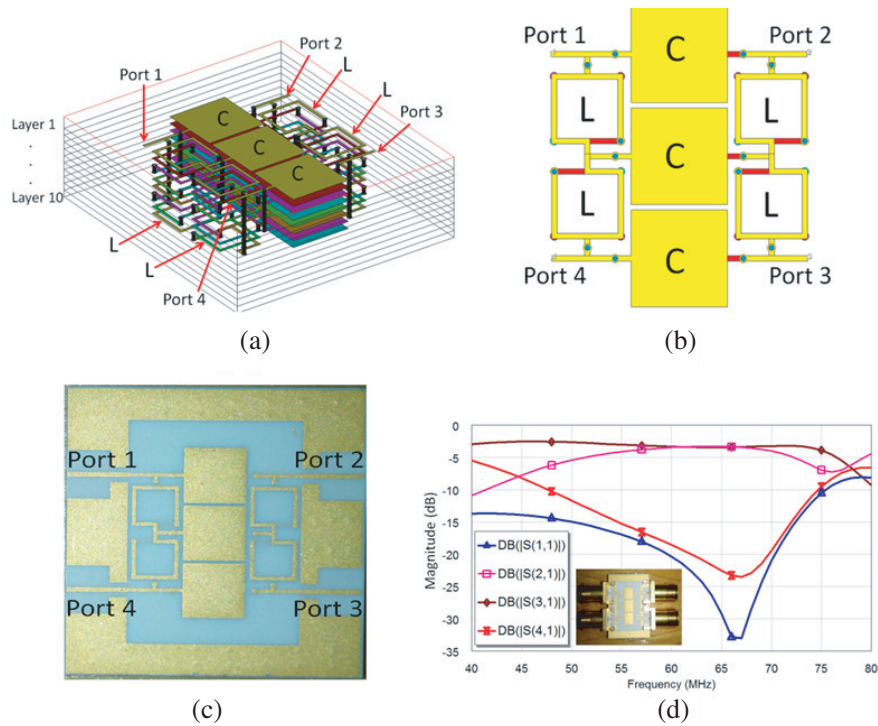


Figure 4. The proposed hybrid. (a) 3D structure, (b) 2D view, (c) photograph and (d) measured S -parameters.

quadrature hybrid is needed to combine two outputs of IRM. The proposed hybrid is designed in a 10-layered LTCC substrate. The circuit topology is shown in Figure 3. Figure 4 shows the structure and performance of the proposed hybrid.

2.4. IF Band Filter Design IF Band BPF Design

BPF working at dozens of 60 MHz frequencies requires very large resonator capacitance and inductance. However, the maximum capacitance and inductance achieved in prior articles [12–15] did not exceed 5 pF and 10 nH, respectively. It is impossible to make components at extremely low frequencies. Having larger capacitances and simultaneously reducing filter size is only possible by using vertically-interdigital-capacitor (VIC).

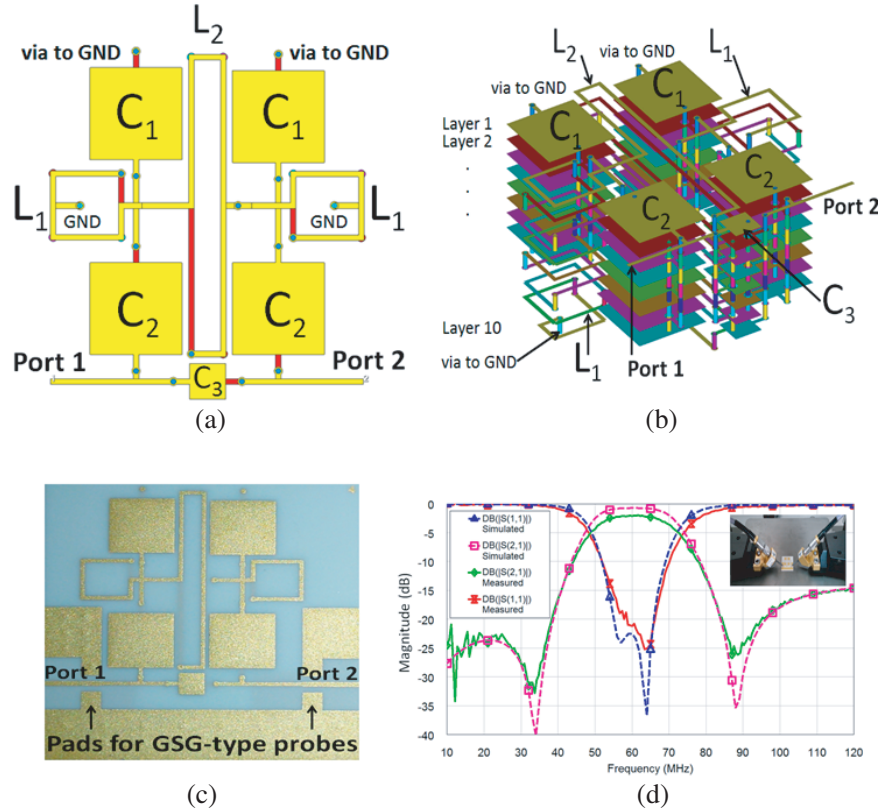


Figure 5. The proposed IF band BPF. (a) 2D structure, (b) 3D view, (c) photograph and (d) measured S -parameters.

An IF band BPF is designed in a 10-layered LTCC as well. Figure 5 shows the structure and performance of the proposed IF band BPF. The simulated results agree well with the measurements. The center frequency is 60 MHz and the bandwidth based on a return loss of 15 dB is 15 MHz. Two finite zeros are located at the prescribed locations. A higher measured passband insertion loss of 1.95 dB is noticeable which is attributed to the greater surface roughness of top metal layer with higher resistive loss. The size of the proposed BPF is only $10 \times 10 \times 1$ mm (without pads for GSG probes), which is equivalent to $0.004 \times 0.004 \times 0.0004\lambda_g$, where λ_g is the guided wavelength on a 1-mm thickness (10 layers) Ferro-A6 substrate at 60 MHz.

2.5. Overall Layout

As all passive components are designed, the next step is to interconnect all active and passive components according to the system diagram in Figure 1. The complete receiver is also assembled in a 10-layer LTCC

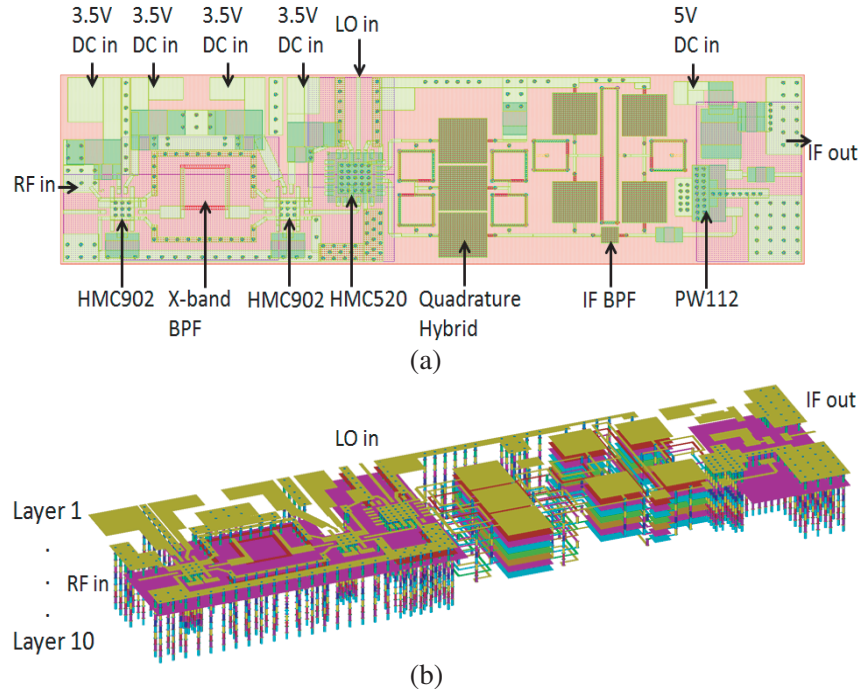


Figure 6. Overall receiver layout. (a) Planar view and (b) 3D view.

substrate. Each LTCC layer has a post-fired thickness of 0.1 mm in Ferro-A6 material with a dielectric constant of 5.9 and loss tangent of 0.002. Figures 6(a) and (b) show the planar view and 3D view of the proposed receiver, respectively. The input port is at the left side and output port at the right side. And the local oscillation (LO) port and DC feed ports are placed on the top side. Figures 7(a) and (b) show the fabricated LTCC board and receiver module after assembly, respectively. The size of the receiver module is only 54 mm × 15 mm × 1 mm. After chips mounting and cavity assembled on the LTCC board, the receiver module needs to be heated for 20 minutes at the temperature of 130°C to guarantee that the paste adhesive works well, and interconnections between chips and microstrips need to be checked using microscope to avoid circuit short. The heating device and microscope are shown in Figure 8.

3. RECEIVER MODULE MEASUREMENTS

Measurement setups use Agilent E8257D PSG, E4447 PSA and Agilent N8975A NFA, shown in Figure 6. And measured results are summarized in Table 1. As shown in Table 2, the measured gain, noise figure (NF) and image rejection are better than 51, 2.5 and 37 dB in the working band, respectively. The measured results meet the requirements of the receiver.

Table 1. Measured results.

Frequency (GHz)	8.5	8.7	9	9.3	9.5
Gain (dB)	51.1	51	51.2	51.2	51.1
NF (dB)	2.5	2.4	2.5	2.4	2.5
Image Rejection (dB)	37.1	37	37.1	37.1	37.1

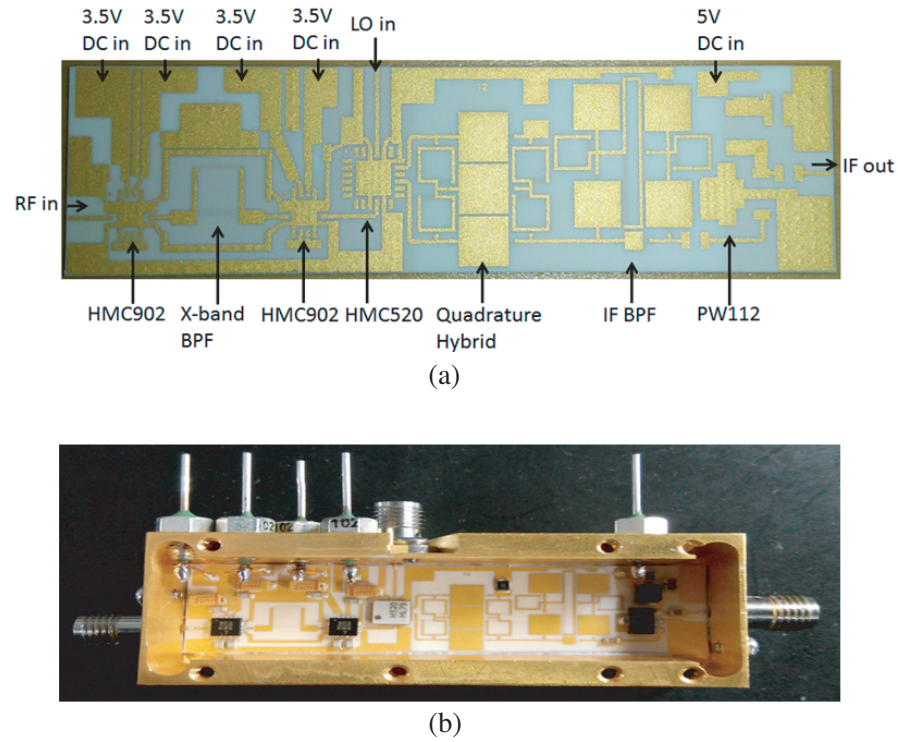


Figure 7. Photograph of the LTCC receiver. (a) Fabricated LTCC board and (b) receiver module after mounting and assembly.

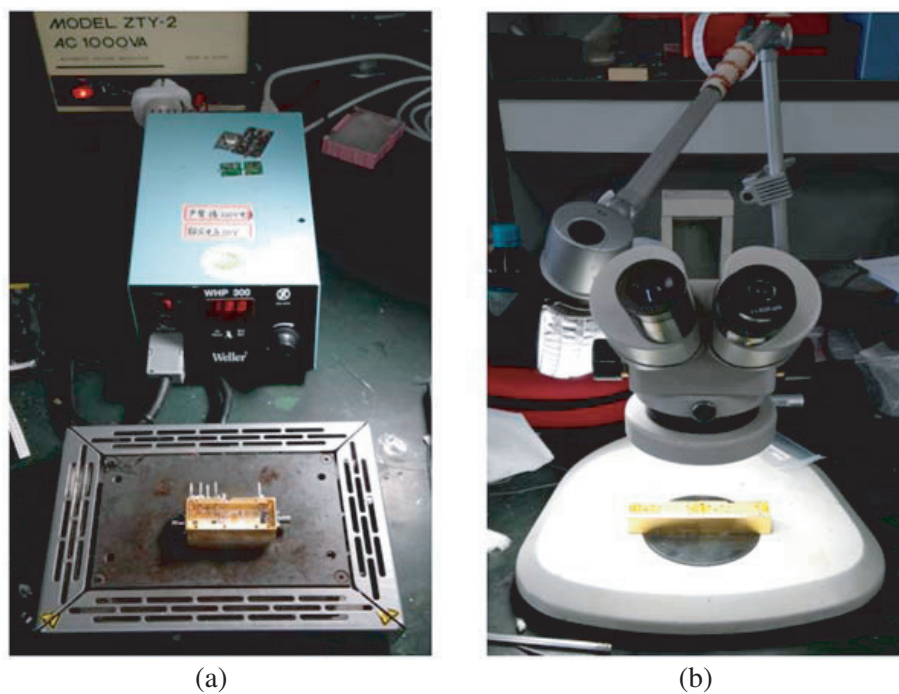


Figure 8. Photographs of (a) heating device and (b) inspection device.

Table 2. Performance comparisons.

Ref.	Frequency (GHz)	Cavity Size (mm ³)	Gain (dB)	NF (dB)
[4]	5	65 × 19.2 × 11	41.3	3.4
[5]	26	55 × 30 × 19	56	4.1
[6]	35	58 × 50 × 22	24	9
This work	9	54 × 15 × 1	51	2.5

4. COMPARISONS AND DISCUSSIONS

Size and performance comparisons with other LTCC implementations are also performed. The proposed LTCC receiver has the smallest size, lowest noise figure and highest gain among [4–6], shown in Table 2.

5. CONCLUSION

Three passive microwave components are proposed and integrated into a 10-layer LTCC receiver module with high integration. The overall size of the receiver module is only 54 mm × 15 mm × 1 mm. The measured gain parameter of the proposed receiver is higher than 51 dB, and noise figure and image rejection are better than 2.5 dB and 37 dB in the working band, respectively. Comparisons and discussions are also carried out.

ACKNOWLEDGMENT

The study was supported by the National Natural Science Foundation of China (Grant No. 61601239), Natural Science Foundation of Jiangsu Province of China (Grant No. BK20160906), China Postdoctoral Science Foundation (Grant No. 2016M601858), Postdoctoral Science Foundation of Jiangsu Province of China (Grant No. 1601030B) and Nanjing University of Posts and Telecommunications Foundation NUPTSF (Grant No. NY215005).

REFERENCES

1. Zhu, L. Z., X. B. Wei, P. Wang, S. Ma, Z. Y. Zeng, and B. C. Yang, “Compact LTCC module for WLAN RF front-end,” *IEEE International Conference on Computational Problem-Solving (ICCP)*, 387–389, 2011.
2. Seki, T., K. Nishikawa, Y. Suzuki, I. Toyoda, and K. Tsunekawa, “60 GHz monolithic LTCC module for wireless communication systems,” *IEEE 9th European Conference in Wireless Technology*, 376–379, 2006.
3. Naghib-Zadeh, H., T. Rabe, J., Toepfer, and R. Karmazin, “Co-firing of LTCC modules with embedded ferrite layers,” *IEEE 18th European Microelectronics and Packaging Conference (EMPC)*, 1–6, 2011.
4. Giordani, R., M. Amici, A. Barigelli, F. Conti, M. D. Marro, M. Feudale, and A. Suriani, “Highly integrated and solderless LTCC based C-band T/R module,” *IEEE European Microwave Conference (EuMC)*, 1760–1763, 2009.
5. Wolff, I., “From antennas to microwave systems — LTCC as an integration technology for space applications,” *IEEE 3rd European Conference on Antennas and Propagation*, 3–8, 2009.
6. Xia, L., R. Xu, and B. Yan, “LTCC-based highly integrated millimeter-wave receiver front-end module,” *International Journal of Infrared and Millimeter Waves*, Vol. 27, No. 7, 975–983, 2006.
7. Bucci, O. M., T. Isernia, and A. F. Morabito, “Optimal synthesis of circularly symmetric shaped beams,” *IEEE Transactions on Antennas and Propagation*, Vol. 62, No. 4, 1954–1964, 2014.

8. Huang, X. D. and C. H. Cheng, "A novel microstrip dual-mode bandpass filter with harmonic suppression," *IEEE Microwave Wireless Compon. Lett.*, Vol. 16, 404–406, 2006.
9. Deng, H. W., Y. J. Zhao, W. Chen, B. Liu, and Y. Y. Liu, "Wide upper-stopband microstrip bandpass filter with dual-mode open loop stepped-impedance resonator and source-load coupling structure," *Microwave Opt. Tech. Lett.*, Vol. 54, 1618–1621, 2012.
10. Jeon, B. K., H. Nam, K. C. Yoon, B. W. Jeon, Y. W. Kim, and J. C. Lee, "Design of a patch dual-mode bandpass filter with second harmonic suppression using open stubs," *IEEE Microwave Conference Proceedings (2010 APMC)*, 1106–1109, 2010.
11. Ohta, I., X. P. Li, T. Kawai, and Y. Kokubo, "A design of lumped-element 3 dB quadrature hybrids," *IEEE Asia-Pacific Microwave Conference Proceedings (1997 APMC)*, 1141–1144, 1997.
12. Hou, J.-A. and Y.-H. Wang, "A compact quadrature hybrid based on high-pass and low-pass lumped elements," *IEEE Microwave Wireless Compon. Lett.*, Vol. 17, 595–597, 2007.
13. Lim, J.-H., D.-Y. Jung, C.-S. Park, and S.-W. Hwang, "Implementation of a 5 GHz LTCC bandpass filter using vertically-interdigitated capacitor and via engineering," *Microw. Opt. Technol. Lett.*, Vol. 50, No. 2, 339–341, Feb. 2008.
14. Huang, H.-H., C.-H. Chen, and T.-S. Horng, "Quasi-lumped bandpass filter with sharp transition edge and wide stopband rejection," *Electron. Lett.*, Vol. 49, No. 7, 479–480, 2013.
15. Brzezina, G., L. Roy, and L. MacEachern, "Design enhancement of miniature lumped-element LTCC bandpass filter," *IEEE Trans. Microw. Theory Tech.*, Vol. 57, No. 4, 815–823, Apr. 2009.
16. Hwang, S., S. Min, M. Swaminathan, V. Sundaram, and R. Tummala, "Thin-film high-rejection filter integration in low-loss organic substrate," *IEEE Trans. Compon., Packag. Manufact. Technol.*, Vol. 1, 1160–1170, Aug. 2011.